JOURNAL OF MATERIALS SCIENCE **36** (2001) 1161 – 1172

Materials for lower temperature solid oxide fuel cells*

J. M. RALPH‡, A. C. SCHOELER, M. KRUMPELT
Electrochemical Technology Program, Argonne National Laboratory, 9700 S. Cass Ave., Argonne, IL 60439, USA
E-mail: ralph@cmt.anl.gov

The solid oxide fuel cell (SOFC) continues to show great promise for the generation of electricity for an increasing range of applications. The present SOFC technology is based on an all-ceramic design, which eliminates the corrosion problems associated with fuel cells containing liquid electrolytes. To obtain good electrochemical performance with the currently used materials, this all-ceramic fuel cell operates at 1000°C. Despite a significant amount of research and several successful demonstrations at the 100 kW level, commercialisation of the technology is not as rapid as anticipated. This is, in part, due to the high operating temperatures required, necessitating the use of expensive materials. As a result of these problems, there has been an effort over the past few years to lower the SOFC operating temperature. This paper will address the issues concerning the development of new materials that can operate at lower temperatures. Many of these issues have been or are being addressed in the research performed at Argonne National Laboratory, and some recent results will be discussed.

1. Introduction

The solid oxide fuel cell (SOFC) continues to attract interest as a potentially reliable, durable and inexpensive technology for generating electricity from hydrocarbon fuels. Compared to the polymer electrolyte fuel cell (PEFC), the fuels processing is much simpler.

The three major designs of SOFC developed into stacks include: tubular [1], planar [2] and monolithic [3]. At present, only the tubular and planar designs are being investigated, although each of these has a number of different configurations [2, 4, 5]. The tubular design has been developed the furthest, mainly due to the efforts of Westinghouse Electric Corp. (now known as Siemens Westinghouse Power Corp.), with stacks built to provide 100 kW of electricity [1]. A future project will provide 250 kW of power with a hybrid stack-gas turbine combination [1]. The planar concept is still favoured by the majority of research labs because of the higher power densities achievable. Major problems with this design include sealing the stacks to prevent fuel and oxidant gases mixing and the thermal mismatch between ceramic components, which has led to cracking during thermal cycling.

Historically, the SOFC was intended for stationary electricity generation due to the brittle nature of ceramic materials, their low impact toughness, and their low resistance to vibration and thermal shock. Despite these shortcomings, companies such as Global Thermoelectric and here at Argonne National Laboratory (ANL), are now developing the SOFC as an auxiliary power unit for the automotive industry [6]. For stationary applications, there is still a split between using the SOFC for larger scale utility base-load applications (e.g., the Siemens Westinghouse design), or the recently preferred choice of smaller distributed electricity sources for individual homes and buildings [7]. Whatever market fuel cells eventually break into, the potential returns remain very large for a successful product.

The state-of-the-art SOFC cell comprises four ceramic components. An yttria-stabilised zirconia (YSZ) electrolyte, a strontium-doped lanthanum manganite (LSM) cathode, a Ni-YSZ cermet anode, and a strontium-doped lanthanum chromite interconnect or bipolar plate. Typically, the cathode is selected as a supporting layer in the tubular design, whereas the electrolyte has been the more common choice for the support in the planar design. The anode is also being considered as the support for the planar design [8]. Many different manufacturing techniques are used to produce each of the ceramic layers, and most have been discussed by Minh [9]. Another major component in fuel cell stacks is the sealant. Many of the sealants are proprietary, and so detailed composition data are not

‡ Author to whom all correspondence should be addressed.

available in the literature, but most sealants are glass, ceramic, or glass-ceramic based.

As with all fuel cells, the SOFC has a number of problems that need to be solved before a commercial product is viable. At present, tests of larger scale stacks (>1 kW) have been performed around 1000°C. These high temperatures prevent the use of plastic or steel for manifolding, piping, heat exchangers, blowers, etc., necessary for a complete fuel cell system. Instead, fuel cell developers have had to use expensive alloys or expensive processes for ceramic production, which are clearly undesirable because they increase fuel cell costs. The high temperature also increases the rate of interfacial reaction between the various ceramic layers, which may affect the longer term performance of the stack, and also raises problems of finding a sealant that is capable of withstanding thermal cycling without cracking. The high temperature is necessary to achieve sufficient oxide-ion conductivity in the YSZ electrolyte layer of each cell. For the planar electrolyte-supported design, the thickness of the electrolyte ranges between 100 and 200 μm. The material used and its thickness determine the required operating temperature.

A monolithic design of SOFC was first proposed in the early 1980's at Argonne National Laboratory (ANL) [10]. More recent SOFC studies at ANL have investigated a variety of glass-sealant materials, adaptable over a wide temperature range [11]; low-temperature SOFCs using ceria-based electrolytes [12]; cathode materials for lower temperature operation; metallic bipolar plates; and sulfur-tolerant anodes. These topics will be discussed further in subsequent sections.

The remainder of this paper will examine each of the components of the SOFC, namely, the electrolyte, cathode, anode, bipolar plate, and sealants, with respect to their development for lower temperature operation. Some recent results from research at ANL on lower temperature cathodes will be included.

2. Electrolyte materials

2.1. Stabilised zirconia

The porous nature of the cathode and anode exposes the electrolyte material to both oxidising and reducing conditions during operation. The main function of the electrolyte is to transport oxygen ions from the cathode to the anode, and as such, it must be a purely ionic conductor and stable in both atmospheres. The first and only practical material that has fully met these requirements is the stabilised-zirconia electrolyte, most commonly doped with yttria (YSZ) [9]. Not only does YSZ fulfill the electrical requirements for a SOFC, but it also has good high-temperature mechanical properties for a ceramic. The mechanical properties of zirconia have been extensively covered in the literature [13].

Previous SOFC designs have required operating temperatures around 1000°C to obtain sufficient conductivity within the electrolyte. Newer SOFC designs are concentrating on reducing the thickness of the YSZ layer, such that a similar resistance can be achieved at lower temperatures. A number of techniques can be used to produce thinner YSZ electrolytes (10–50 μm) [14–16], but the successful technique must be capable of scale-up for the mass market.

With the development of thinner electrolytes, the supporting structure in a number of cell designs had to change, with the anode as the preferred choice for most [8]. However, there are certain theoretical and practical limitations to the reduction in thickness that can be achieved. Steele [17] recently discussed the effect of electrolyte thickness on the surface exchange and diffusion coefficient of oxygen. At a certain thickness the surface exchange reaction and not the diffusion of oxygen becomes the rate-limiting step, and thus further reduction in thickness serves no benefit. From a practical standpoint, below about 1 μm it is difficult to produce thin films without forming small pinholes or cracks, through which cross-mixing of gases can occur and thereby lower the power density for the SOFC [9]. It is unlikely, therefore, that YSZ-based SOFC stacks will operate below about 700°C because the resistance of YSZ becomes too high [18].

2.2. Alternative electrolytes

Instead of reducing the thickness of the electrolyte, another solution would be to develop a new material with a higher oxygen-ion conductivity compared to YSZ. Three materials are known to have a higher conductivity in air: bismuth oxide, doped ceria, and doped lanthanum gallate. Of all ceramic electrolytes δ-Bi_2O_3 exhibits the highest oxygen-ion conductivity (approximately 1 Scm^{-1} at 750°C [19]) due to its extremely open crystal structure. This structure is only stable above 729°C, but it is possible to stabilise a low-temperature form by doping with Y_2O_3 or Er_2O_3. At relatively high oxygen partial pressures, the most dominant problem for all the bismuth-based electrolytes is the reduction of Bi^{3+} to metallic Bi, which effectively destroys the electrolyte [20]. It is unlikely that any bismuth-based electrolyte can be developed to withstand the reducing conditions in an SOFC.

Ceria doped with alkaline earths or rare earths has received considerable attention over the past two decades [21]. The ionic conductivity of this material is well established for gadolinia- and samaria-doped ceria; these dopants have been shown to produce the highest conductivities in ceria (approximately 0.1 Scm^{-1} at 700°C [17]). Although doped ceria is more stable than bismuth oxide, in reducing conditions ($pO_2 = 10^{-19}$ atm) the Ce^{4+} reduces to Ce^{3+}, introducing electronic conductivity according to Equation 1, which uses Kröger-Vink notation [22].

$$O_O^x \leftrightarrow V_O^{\bullet\bullet} + \tfrac{1}{2}O_{2(g)} + 2e' \qquad (1)$$

The electronic conductivity acts as a short-circuit pathway through the electrolyte and effectively reduces the SOFC efficiency. The range of oxygen partial pressures over which the electrolyte is predominantly ionic widens as the temperature is reduced. Below 700°C, the degree of electronic conductivity is thought to be low enough to allow acceptable SOFC operation [12]. Further, the performance of the ceria electrolyte

is improved when current is actually drawn from the cell [12].

Measurements performed at Imperial College on single cells at 650°C have obtained power densities around 170 mW cm^{-2} for a gadolinia-doped ceria (CGO) electrolyte that is 5 μm thick [23]. Similar studies at ANL on cells operating at 500°C have obtained power densities of 140 mW cm^{-2} for a CGO electrolyte that is 30 μm thick [12]. To date, this is the highest performance of a SOFC at 500°C. The Lawrence Berkeley National Laboratory has also demonstrated good SOFC performance using CGO and samaria-doped ceria (CSO) electrolytes. Power densities of 350 mW cm^{-2} at 600°C were achieved in cells using a 10 μm-thick electrolyte [24]. Testing of single cells and five-cell stacks by Honegger *et al.* [25] showed stable performance for over 2000 hours. An average power density of 125 mW cm^{-2} at 650°C was achieved with a 200 μm thick CGO electrolyte. These power densities are somewhat lower than those obtained for the zirconia electrolytes operating between 800 and 1000°C (>1000 mW cm^{-2} for single cells and >600 mW cm^{-2} for stacks [26]), so there is still a considerable room for improvement. Correct selection of electrodes and electrode deposition techniques will all play significant roles. For low temperature operation (500–700°C), doped-ceria electrolytes remain the only candidate material, but larger scale stacks will need to be tested before this electrolyte can be adopted.

The newest electrolyte material under development is a lanthanum gallate system. This material differs from the former electrolytes because it is based on a perovskite lattice (ABO_3) rather than a fluorite or fluorite-related lattice (AO_2). The perovskite lattice is less open than the fluorite lattice, but surprisingly, the conductivity of lanthanum strontium gallium magnesium oxide ($La_{0.9}Sr_{0.1}Ga_{0.8}Mg_{0.2}O_3$, referred to as LSGM) is higher than that of the doped-zirconia electrolytes [27, 28]. The target operation temperature for this material is around 800°C, but further development of the cathode and anode materials is needed. Also, the long-term stability of the electrolyte working with some of the candidate fuels has yet to be demonstrated and there are some concerns regarding the high creep rate of this material compared to YSZ [29].

Recently, the price of scandium oxide has fallen sharply due to an influx from the Russian market. Scandia-doped zirconia exhibits conductivity several times that of YSZ and may extend the use of zirconia electrolytes to lower temperatures [30]. The availability and cost of scandia remains a concern and may limit future use of this material.

3. Cathode materials

3.1. Doped lanthanum manganite

The development of cathode materials in SOFCs has mainly focussed on the doped lanthanum manganite system because this material remains stable in oxidising atmospheres, has sufficient electrical conductivity at 1000°C, and has a close thermal expansion match to the YSZ electrolyte. Generally, the cathode fabrication is the final step in the cell manufacture to avoid interfacial reactions between the electrolyte and cathode, which occur rapidly at temperatures above 1200°C, to form $La_2Zr_2O_7$ [31, 32]. The most common dopant used is strontium due to its good size match to lanthanum. The strontium dopant does not increase the oxygen vacancy concentration, a common phenomenon in most of the other perovskite cathode materials studied, but rather oxidises the manganese ion according to Equation 2.

$$SrO \xrightarrow{LaMnO_3} Sr'_{La} + Mn^{\bullet}_{Mn} + O^{X}_{O} \qquad (2)$$

This reaction effectively increases the electron-hole concentration and improves the electrical conductivity. The absence of oxygen vacancies in LSM results in a conductivity that is almost exclusively electronic. This restricts the reduction of oxygen to the three-phase boundary regions, where the air, cathode, and electrolyte are in intimate contact. This restriction is the primary reason why LSM does not have acceptable performance at lower temperatures, where the entire cathode surface participates in the reduction and transport of oxygen to the electrolyte. While some uncertainty exists over the actual oxygen vacancy concentration in LSM and the mechanisms that introduce it, this concentration is unquestionably low [33].

The electronic conductivity of LSM increases approximately linearly with increasing Sr concentration up to a maximum around 50 mol% [34]. Unfortunately, for Sr concentrations above about 30 mol%, the cathode reacts with the YSZ electrolyte to form $SrZrO_3$ [35]. Both $La_2Zr_2O_7$ and $SrZrO_3$ have high electrical resistances and are undesirable phases at the interface. Therefore, LSM compositions have Sr concentrations of 10–20 mol%.

Two approaches have been taken to improve the performance of LSM cathodes so that they may be used at lower temperatures. The first is to add a second ionically conducting phase to LSM to extend the surface area over which the oxygen reduction reaction can occur. Several groups are showing very good performances using a LSM-YSZ cathode [36–38] but it is not clear how low in temperature these cathodes can operate.

The second approach has been to dope LSM with an ion that promotes the formation of oxygen vacancies when strontium is doped on the A-site. Research in this area has been performed at ANL, where both gallium and aluminium doping onto the B-site appear to enhance the performance of the cathodes [39]. Gallium and aluminium both have strong preferences for tetrahedral coordination in perovskites. There presence provides an alternative to Mn oxidation and may help stabilise a small number of vacancies in the perovskite lattice (the black tetrahedron in Fig. 1). In addition, at low doping levels vacancies are also in the coordination spheres of the adjacent manganese cations (the darker grey square pyramids in Fig. 1), a situation consistent with its known defect chemistry.

While both approaches appear to improve the performance of LSM, it is unlikely that these cathode materials will operate below 800°C. The research at ANL is now focussing on non-manganese systems that show inherent mixed conductivity.

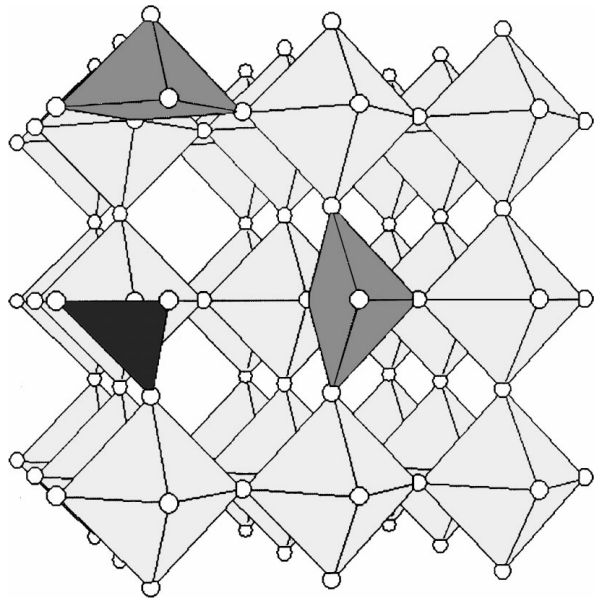

Figure 1 A model for the local defect structure created by addition of a tetrahedral cation to the LSM perovskite framework. Light grey polyhedra represent [MnO_6] octahedra, darker grey polyhedra represent the singly oxygen deficient [MnO_5] square pyramids, and the black tetrahedron represents the dopant tetrahedral cation [MO_4]. The small open spheres are oxygen anions. The A-site (La or Sr) cations have been eliminated for clarity.

3.2. Alternative cathode materials

There have been many cathode compositions evaluated for use on YSZ at 1000°C but most have reacted with YSZ or decomposed at this temperature. The lanthanum cobaltates have been studied extensively at lower temperatures (500–700°C) using the ceria-based electrolytes, but it is known that ceria does not react with the cobaltates. There appears to be a relatively limited number of studies on cathode materials with YSZ at lower temperatures (650–850°C) and, at present, no standard material has been identified to replace LSM. Research currently being performed at ANL is targeted at re-evaluating cathode materials that were discounted at higher temperatures and to explore new materials, both for CGO and YSZ electrolytes.

3.3. Research performed at ANL

Several first-row transition metals substituted for the manganese ion form perovskites that have much higher electronic and ionic conductivities [40, 41]. The transition metals Co, Fe, Ni, Cu, and combinations thereof have all been studied to varying degrees (Cr has also been studied but its properties are worse than Mn). These studies have revealed problems with thermal expansion, reactivity, and the stability of the cathode itself at 1000°C [41, 42]. With the shift to lower operating temperatures, these problems become less severe, and some of the materials that were discounted for use at higher temperatures are now being re-examined at ANL.

Two electrolyte systems are being considered at ANL : CGO for operation at 500–700°C and YSZ for operation at 650–850°C. For CGO electrolytes, there have been no reports of reactions with any of the perovskite electrodes studied, permitting the highly conducting cobaltate systems to be evaluated. Several layered cuprates have also been studied, although their long-term stability is uncertain. The areal resistances (also referred to as area specific resistances, ASR) of these cathode materials have been compared to those of the most commonly used cathode material on CGO, $La_{1-X}Sr_XCo_{1-Y}Fe_YO_3$, referred to as LSCF. The same compositions have also been tested on YSZ. Table I in Section 3.3.2 lists the cathode materials tested on CGO and YSZ.

Some reports in the literature suggest that replacing lanthanum on the A-site can lead to lower interfacial resistances for the perovskites on YSZ [43, 44]. Most of the candidate materials contain rare earth elements due to the geometric constraints placed on the A-site. Two approaches have been considered to reduce the interfacial resistance.

Most of the published work on alternative A-site cations is focussed on YSZ electrolytes, but the theories can generally be adapted for CGO as well. The first approach suggested to improve the interfacial resistance is to choose a cation that doesn't form a stable insulating phase with the YSZ electrolyte. Lanthanum-based cathodes commonly form $La_2Zr_2O_7$ at the interface, which has a high resistance and rapidly degrades the performance of the cathode. Although making A-site deficient cathodes has made some improvement in this situation, lanthanum zirconate is still detected, especially in the non-manganite systems. Alternative cations include Gd, Nd and Y [43, 44], however, Nd

TABLE I Prepared cathode compositions and their reactivity with YSZ and CGO electrolytes

	Reaction Products	
Composition	With YSZ	With CGO
$La_{0.8}Sr_{0.2}CoO_3$	$La_2Zr_2O_7$, $SrZrO_3$	none
$La_{0.8}Sr_{0.2}Co_{0.8}Ni_{0.2}O_3$	$La_2Zr_2O_7$, $SrZrO_3$, NiO	none
$La_{0.8}Sr_{0.2}Co_{0.8}Fe_{0.2}O_3$	$La_2Zr_2O_7$, $SrZrO_3$	none
$La_{0.8}Sr_{0.2}Co_{0.8}Ni_{0.15}Cu_{0.05}O_3$	$La_2Zr_2O_7$, $SrZrO_3$	none
$Sm_{0.8}Sr_{0.2}CoO_3$	$Sm_2Zr_2O_7$, $SrZrO_3$	none
$La_{0.8}Sr_{0.2}FeO_3$	none	none
$La_{0.8}Sr_{0.2}Fe_{0.8}Ni_{0.2}O_3$	$La_2Zr_2O_7$, $SrZrO_3$	none
$La_{0.8}Sr_{0.2}Fe_{0.8}Ni_{0.15}Cu_{0.05}O_3$	$La_2Zr_2O_7$, $Sr_2Fe_2O_5$	none
$LaNiO_3$	$La_2Zr_2O_7$, La_2NiO_4, NiO	La_2NiO_4, NiO
$Nd_{0.8}Sr_{0.2}CoO_3$, $Gd_{0.8}Sr_{0.2}CoO_3$,$La_{0.8}Sr_{0.2}Fe_{0.8}Co_{0.2}O_3$, $YBa_2Cu_3O_7$, $Bi_2Sr_2CaCu_2O_8$	Not measured	Not measured

shows limited improvement and forms a more stable pyrochlore [45]. Gadolinium is reported to not form a stable pyrochlore phase with zirconium, while yttrium is a constituent of the YSZ electrolyte and thus should not cause any interfacial problems.

The second approach is to choose a cation with multiple valences in an attempt to improve the electronic conductivity of the cathode material. Two cations previously studied are Sm (+2 and +3) and Pr (+3 and +4) [46, 47]. Two other cations that could be considered are Ce and Tb (both +3 and +4), although cost may eliminate the use of Tb.

The studies so far have only concentrated on one or two cations at a time. As discussed in Section 3.3.1. and 3.3.2. a number of these materials have been made and tested, in an identical manner, to obtain a true comparison among the different cations. The cations chosen were Gd, Sm, and Nd, with La as the reference.

The CGO electrolyte is much less considered in the literature. The problems with a pyrochlore phase forming at the interface do not occur for the ceria-based electrolytes, and thus, one would expect any improvement from changing the A-site to be small. A seemingly obvious choice for an alternative cation is Gd, use of $Gd_{0.8}Sr_{0.2}CoO_3$ on CGO is not reported in the literature.

3.3.1. Experimental procedures

To standardise the testing procedures in the present work at ANL, the A-site dopant was always Sr at a doping concentration of 20 mol%. This level was chosen to minimise the formation of $SrZrO_3$ and to allow comparison with the majority of the literature studies. The B-site cation (Co, Fe or Ni) was also doped with another cation (Co, Fe, Ni or Cu). The dopant concentration was fixed at 20 mol%, except for Cu, which was fixed at 5 mol%. The 20 mol% concentration was considered sufficiently high to observe any interfacial resistance differences. Copper was doped at a lower concentration because of the possibility of forming a lower temperature eutectic with the alkaline earth metals. The two layered cuprates ($YBa_2Cu_3O_7$ and $Bi_2Sr_2CaCu_2O_8$) were obtained commercially (Aldrich Chemical Company).

All cathode compositions, except the layered cuprates and $Gd_{0.8}Sr_{0.2}CoO_3$, were prepared using the glycine-nitrate process and calcined at 1250°C. The two cuprates, which were obtained commercially, received no calcination treatment, while $Gd_{0.8}Sr_{0.2}CoO_3$ was calcined at 1150°C due to partial melting at 1250°C. All powders were then milled for 7 days in ethanol, using zirconia media, to form the cathode inks. Each of the cathode inks was then slurry coated onto YSZ (obtained from Performance Ceramics) and CGO (prepared in-house) disks and sintered at 1000°C for 1 hour. The electrode pattern is shown in Fig. 2. This procedure was repeated on the reverse side of the disks.

The reactivity of each cathode material with the respective electrolyte was evaluated by mixing 50% by volume of each of the powders with the electrolyte powder and then pressing the mixture into a pellet. The pellets were then annealed for one week at 1200°C. X-ray diffraction was used to determine the presence of any reaction products.

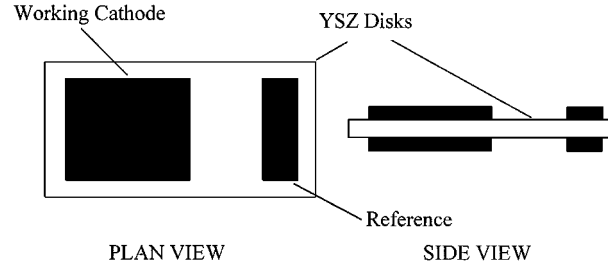

Figure 2 Electrode pattern used for electrically screening cathode compositions.

Each cathode was then evaluated electrically using three-probe impedance spectroscopy at 50°C increments over the required operating temperature range. The reference electrodes allowed the cathode areal resistance to be separated from the electrolyte resistance. Samples prepared in an identical way were also used to perform longer-term tests. Samples were annealed at 650°C and 800°C for CGO and YSZ electrolytes, respectively, for approximately 500 hours. Impedance measurements were recorded with time to evaluate the thermal stability of each cathode. The initial target for these electrodes was to achieve an areal resistance $<1\ \Omega cm^2$.

3.3.2. Results and discussion

The cathode powders were all determined to be single phase using X-ray diffraction; however, the B-site doped nickelates did not have the perovskite structure and were not tested further. The results of the reactivity test are summarised in Table I. It is clear that all of the cobaltate compositions decomposed and reacted with the YSZ electrolyte. The B-site doped ferrates and un-doped nickelate also reacted with YSZ. Only $La_{0.8}Sr_{0.2}FeO_3$ showed no reaction with YSZ. No reactivity was observed for all of the cathode materials with CGO, although the nickelate electrode disproportionated. The reactivity of the layered cuprates has not yet been established.

Figs 3 and 4, show a comparison of the areal resistances for each cathode material on YSZ and CGO electrolytes, respectively. Fig. 3, clearly shows that all the cobaltates and most of the ferrate compositions have areal resistances much greater than the $1\ \Omega cm^2$ target at the highest temperature (850°C). The composition $La_{0.8}Sr_{0.2}Fe_{0.8}Ni_{0.2}O_3$ (LSFN) has an areal resistance just above this value at 850°C, but the resistance increases rapidly as the temperature is reduced (because of its large activation energy, see Table II). The composition $LaNiO_3$ has a value close to $1\ \Omega cm^2$ and because of its low activation energy, the resistance increases proportionately less as the temperature is reduced. Note that this composition has no Sr doping on the A-site, which is normally considered to greatly increase the conductivity in these cathode materials. Successful doping on the B-site may further

TABLE II Interfacial activation energies for cathode materials on YSZ and CGO electrolytes, calculated from the areal resistance data

Composition	Interfacial Activation Energy/eV	
	With YSZ	With CGO
$La_{0.8}Sr_{0.2}CoO_3$	1.7	1.7
$La_{0.8}Sr_{0.2}Co_{0.8}Fe_{0.2}O_3$	1.7	2.1
$La_{0.8}Sr_{0.2}Co_{0.8}Ni_{0.2}O_3$	1.9	2.4
$La_{0.8}Sr_{0.2}Co_{0.8}Ni_{0.15}Cu_{0.05}O_3$	1.8	1.7
$Sm_{0.8}Sr_{0.2}CoO_3$	1.7	2.0
$Gd_{0.8}Sr_{0.2}CoO_3$	2.1	1.7
$Nd_{0.8}Sr_{0.2}CoO_3$	2.0	1.8
$La_{0.8}Sr_{0.2}FeO_3$	1.7	1.9
$La_{0.8}Sr_{0.2}Fe_{0.8}Co_{0.2}O_3$	1.7	1.7
$La_{0.8}Sr_{0.2}Fe_{0.8}Ni_{0.2}O_3$	1.9	1.7
$La_{0.8}Sr_{0.2}Fe_{0.8}Ni_{0.15}Cu_{0.05}O_3$	2.1	1.9
$LaNiO_3$	1.3	1.2
$YBa_2Cu_3O_7$	2.0	1.9
$Bi_2Sr_2CaCu_2O_8$	2.8	1.6

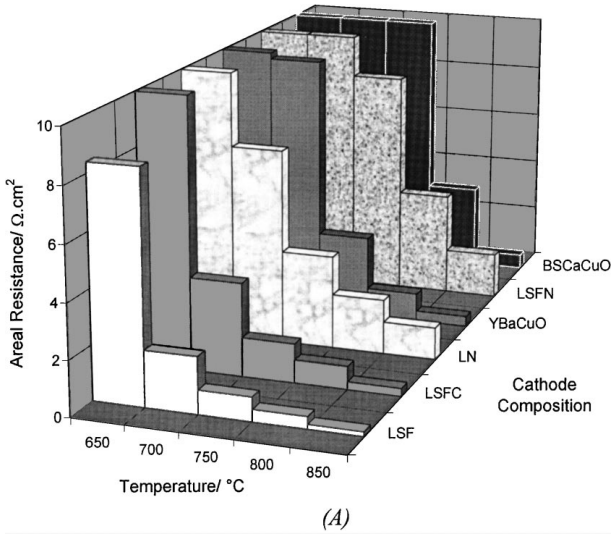

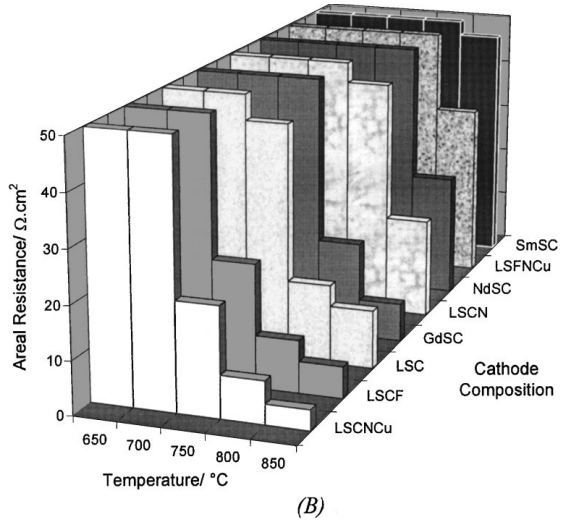

Figure 3 Areal resistance of cathode materials on YSZ electrolytes. (*A*) Shows cathodes with the lowest resistances. Resistances above 10 Ωcm^2 have been truncated for clarity at higher temperature. (*B*) Shows cathodes with the highest resistances. Resistances above 50 Ωcm^2 have again been truncated. Composition names have been abbreviated to the first letter of each cation; element symbols are used for Gd, Sm, Nd, Ca, Ba and Cu.

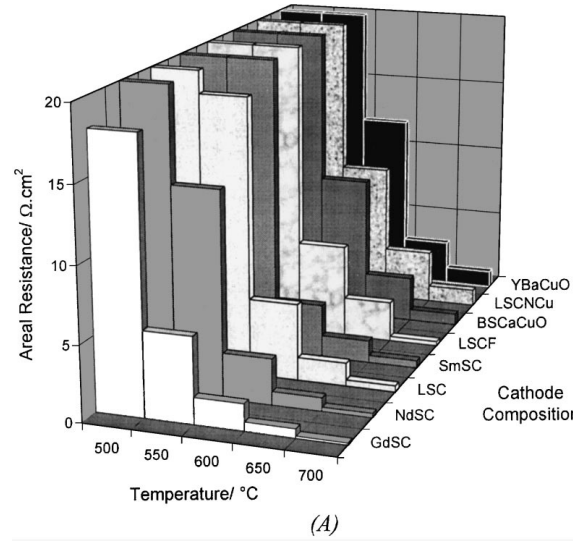

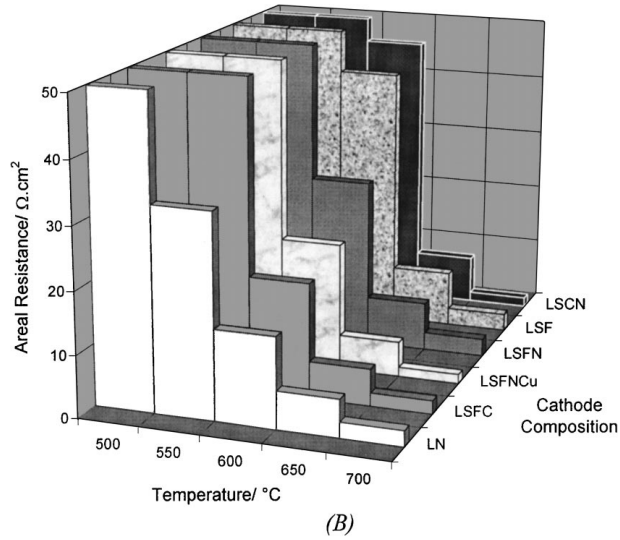

Figure 4 Areal resistance of cathode materials on CGO electrolytes. (*A*) Shows cathodes with the lowest resistances. Resistances above 20 Ωcm^2 have been truncated for clarity at higher temperature. (*B*) Shows cathodes with the highest resistances. Resistances above 50 Ωcm^2 have again been truncated. Composition names have been abbreviated to the first letter of each cation; element symbols are used for Gd, Sm, Nd, Ca, Ba and Cu.

improve the resistance and provide a potential new cathode material. Clearly, the cathode compositions with the greatest performance are $La_{0.8}Sr_{0.2}FeO_3$ (LSF) and $La_{0.8}Sr_{0.2}Fe_{0.8}Co_{0.2}O_3$ (LSFC), which reach areal resistances close to 0.1 Ωcm^2 and 0.3 Ωcm^2 at 850°C, respectively. Repeated tests on $La_{0.8}Sr_{0.2}FeO_3$ confirm an areal resistance much less than 1 Ωcm^2. This material also has a low activation energy, resulting in the areal resistance of $La_{0.8}Sr_{0.2}FeO_3$ remaining below 1 Ωcm^2 down to 750°C. Thus, $La_{0.8}Sr_{0.2}FeO_3$ is a good candidate material for a low temperature cathode.

The layered structures also show good electrical performance at the highest temperatures; however, the lower activation energy of $YBa_2Cu_3O_7$ (YBaCuO) makes this material more suitable for operation as the temperature is reduced. The performance of this layered structure is similar to that of the best perovskite material and could open up a whole new class of potential

cathode materials. To the best of the authors' knowledge, these layered structures have not been used as cathode materials on YSZ before. As a reference, the areal resistance for LSM on YSZ at 1000°C is about 1 Ωcm^2 [48].

The areal resistances for cathodes on CGO, displayed in Fig. 4, show that the cobaltates all achieve performances below or close to 1 Ωcm^2 at 700°C. The standard $La_{0.8}Sr_{0.2}Co_{0.8}Fe_{0.2}O_3$ (LSCF) material performs better than most materials, achieving an areal resistance of 0.3 Ωcm^2 at 700°C; $La_{0.8}Sr_{0.2}CoO_3$ (LSC) also attains a low areal resistance.

Because $La_{0.8}Sr_{0.2}Co_{0.8}Fe_{0.2}O_3$ has a higher activation energy compared to $La_{0.8}Sr_{0.2}CoO_3$ (see Table II), its resistance increases rapidly as the temperature is reduced. Perhaps the most surprising results from this initial screening have been the extremely good performances obtained by all the La-substituted compositions. For example, $Sm_{0.8}Sr_{0.2}CoO_3$ has a performance similar to $La_{0.8}Sr_{0.2}Co_{0.8}Fe_{0.2}O_3$, while $Gd_{0.8}Sr_{0.2}CoO_3$ and $Nd_{0.8}Sr_{0.2}CoO_3$ have much better performances. The areal resistance of $Gd_{0.8}Sr_{0.2}CoO_3$ is approximately 0.1 Ωcm^2 at 700°C and displays the lowest activation energy among all the cobaltates measured. The presence of Gd as one of the main constituents in the cathode also reduces the probability of unfavourable reactions with CGO, which itself contains Gd. Thus, $Gd_{0.8}Sr_{0.2}CoO_3$ appears to be a promising new cathode material for use with CGO.

The layered cuprates again showed good performances. These are the first materials studied that have performed well on both CGO and YSZ electrolytes. Of the cuprates, $Bi_2Sr_2CaCu_2O_8$ (BSCaCuO) displayed a slightly better areal resistance and a lower activation energy, similar to that of $La_{0.8}Sr_{0.2}Co_{0.8}Fe_{0.2}O_3$. This is the first time that this material has been used as a cathode material on CGO and warrants further investigation.

Figs 5 and 6, present the longer-term thermal stability of some of the better-performing cathode materials, identified from the electrical evalutation tests. These experiments were performed at the simulated operational temperatures of 650°C for CGO and 800°C for YSZ. As shown in Fig. 5, $La_{0.8}Sr_{0.2}FeO_3$ displays an extremely stable performance after an initial equilibration time, with an areal resistance below 1 Ωcm^2 and $LaNiO_3$ displays a reasonably stable performance but, as expected, has a higher areal resistance.

As shown in Fig. 6, $La_{0.8}Sr_{0.2}Co_{0.8}Fe_{0.2}O_3$ remains stable for the 500 hours with an areal resistance of 2-3 Ωcm^2. The $Sm_{0.8}Sr_{0.2}CoO_3$ displays a slowly increasing resistance with time, but this behaviour is thought to be more due to a microstructural effect than increased interfacial reactions. The stability of the other A-site substituted cathodes is still to be determined.

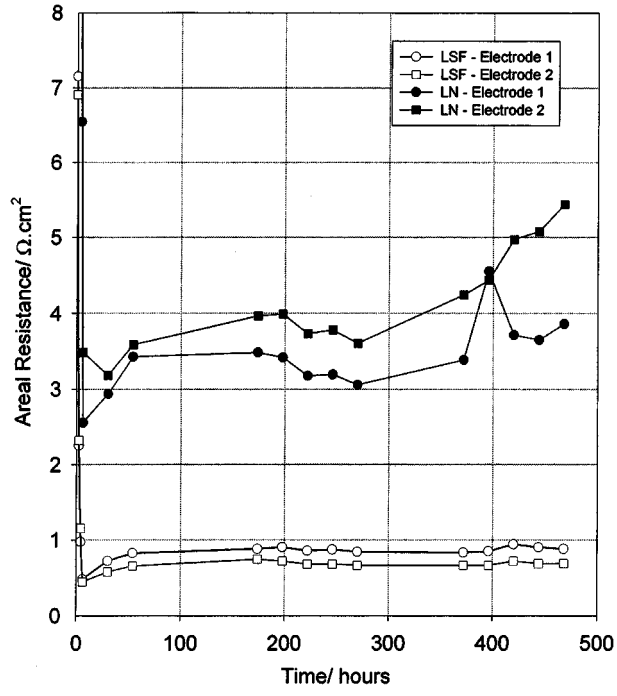

Figure 5 Long-term cathode stability of $La_{0.8}Sr_{0.2}FeO_3$ and $LaNiO_3$ on YSZ in air at 800°C.

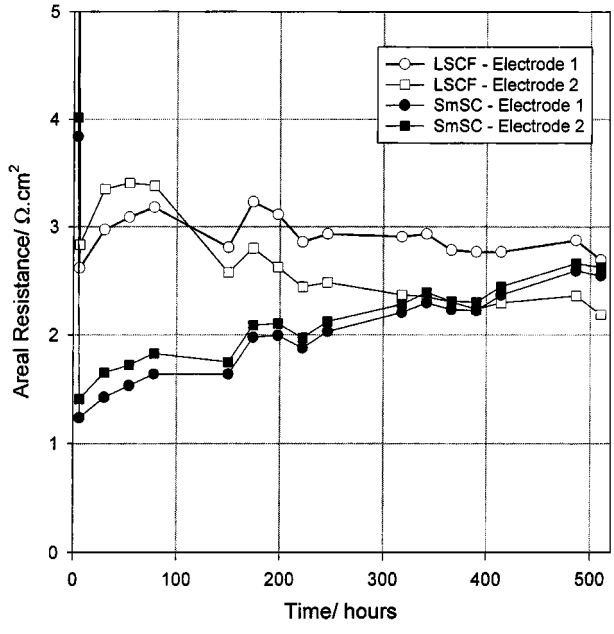

Figure 6 Long-term cathode stability of $La_{0.8}Sr_{0.2}Co_{0.8}Fe_{0.2}O_3$ and $Sm_{0.8}Sr_{0.2}CoO_3$ on CGO in air at 650°C.

4. Anode materials

4.1. Ni-YSZ cermets

Early work in the sixties and seventies singled out nickel and cobalt metals as candidate materials for the anode [49]. The pioneering research performed by Westinghouse Electric Corporation developed the Ni-YSZ cermet in an attempt to better match the thermal expansion coefficients of the anode to the YSZ electrolyte [50]. The anode in the SOFC has remained virtually unchanged since the introduction of the Ni-YSZ cermet and is still used in the majority of SOFC cells and stacks.

The main functions of the anode are to facilitate the adsorption and oxidation of hydrogen from the fuel stream, thus permitting the oxygen ions from the electrolyte to combine with the hydrogen to form water and release electrons to the external circuit. The anode must therefore be predominantly an electronic conductor.

Since YSZ is electronically insulating, the Ni phase in the cermet must be present in a high enough concentration to allow a complete conducting pathway through the anode. This limit has been studied in a number of systems and is commonly known as the percolation threshold and normally occurs around 30 vol% of the conducting phase. The balance between matching thermal expansions and achieving sufficient conductivity has led to the development of anodes with Ni concentrations of 40–60 vol% [51].

Recently, CGO has been tested in place of YSZ in the cermet. A number of groups are now evaluating the benefits and long-term stability of a Ni-[ceria-samaria (CSO)] cermet [52]. When ceria is placed in a reducing environment, Ce^{4+} tends to reduce to Ce^{3+}, as shown previously in Equation 1, which introduces electrons into the ceria lattice. The ceria structure is no longer insulating, like the YSZ phase, and thus should further improve the electrical properties of the anode, while maintaining the Ni microstructure. Of course, CSO does not have an exact thermal expansion match to YSZ, and some undesirable reactivity may occur between CSO and YSZ. These factors will need to be investigated further.

4.2. Choice of fuel

One of the most important decisions that still remains unresolved, and affects all fuel cell types, is the choice of fuel. While hydrogen achieves the best performance in most cells, it is unlikely to be used in the near term because of the difficulties in storing hydrogen and the lack of a widespread distribution network, especially for mobile applications. Alternative fuels that are being looked at more seriously for immediate use are the short-chain liquid hydrocarbons, such as methanol and ethanol [53]. These fuels have the advantage of being liquids and are, therefore, easy to transport. They are also relatively easy to produce and are already manufactured on a large scale. Reforming these fuels is easier and involves less complicated equipment than nonoxygenated hydrocarbons. Perhaps the greatest quality over existing fuels is that these alcohols are renewable fuel sources. However, health concerns, especially for methanol, still need to be addressed; high volatility and the lack of a distribution network are both major disadvantages.

Petroleum (gasoline), diesel, and natural gas (both in gaseous and liquid form) are all being developed as a potential fuel in mobile and stationary applications [54]. These fuels are well accepted by the world's community, and the present extensive infrastructure is a key advantage. Converting petroleum and especially diesel to a hydrogen-rich gas in reformers that potentially may fit under the hood of a vehicle is a great challenge. ANL has been able to develop an autothermal reformer that has been surprisingly effective in converting a broad spectrum of hydrocarbon fuels. A hydrocarbon with the general formula $C_nH_mO_p$ is reacted with x moles of air and $2n\text{-}2x\text{-}p$ moles of water to generate a hydrogen rich gas [55]. Proprietary catalysts are used to support these reactions at about 700°C. At its current state of development, this reactor measures about 20 cm in diameter and is 50 cm long to generate enough hydrogen for a 10 kW fuel cell.

The choice of fuel may well be decided by the end use of the fuel cell. For mobile applications, a liquid fuel is desirable to allow easy handling and transportation. Candidate fuels here would be methanol, ethanol, petroleum, diesel, and liquefied natural gas. For stationary applications, a liquid fuel is not essential, and it is more likely that a central gas pipe network would provide the fuel. Natural gas (predominantly methane) is an obvious choice due to the large reserves available. Methane is also produced as a by-product from a number of processes. For remote or military applications, liquid fuel with a high energy density would be more desirable, and thus, diesel is more likely to be chosen.

Until the fuels for the different applications are chosen, it is difficult to isolate the problems that the fuel will cause. In the short term, petroleum, diesel, or natural gas appear to be the likely fuels selected. All have high sulfur concentrations, which will poison the current anode materials and drastically lower the SOFC performance. Also gaining popularity is naphtha [56]. Naphtha is produced as an intermediate in the refining process of petroleum and does not contain many of the unwanted additives present in petroleum. Naphtha could potentially be cheaper to produce than petroleum because of the fewer steps needed to refine it. Also, its lower sulfur content compared to petroleum should make it easier to remove the sulfur. Naphtha could be used in all present distribution infrastructures with little modification and possesses no extra hazards over that of petroleum.

4.3. Sulfur tolerance

Until recently, the problem of sulfur poisoning of the SOFC anode was not widely accepted. As a result of longer tests on large-scale stacks, it has been determined that the sulfur tolerance of the anode is relatively low (<10 ppm), and higher levels of sulfur quickly degrade the SOFC performance. The current solution to this problem is to use a sulfur-adsorbent zinc oxide bed in the fuel feed, prior to entry into the stack. With fuels such as petroleum, the zinc oxide beds become saturated relatively quickly and need to be changed frequently [57]. The beds add to the complexity and therefore cost of any SOFC system, and thus, developing a sulfur-tolerant anode would be advantageous.

Research on the anode has been much less active compared to other cell components in the SOFC. The overpotential at the anode is much lower than that of the cathode, and the anode also has a good thermal match to the electrolyte, with no degrading long-term reactions. Introducing a few percent of water into the fuel feed stream solved early problems of carbon deposition on the nickel sites. Relatively few new materials have been proposed to replace the Ni-YSZ cermet, and none has proven to match or better its performance, with the possible exception of doped ceria replacing YSZ.

The search for sulfur-tolerant anodes has only just begun. Essentially two approaches are being taken to develop sulfur-tolerant anodes. The first is to choose a material (most likely a metal or alloy) that has a low affinity towards the formation of a sulfide. The material would thus be inert to the sulfur, present as H_2S in the fuel stream, and it would pass through with no interaction with the anode. Unfortunately, most of the candidate materials are precious metals and were eliminated from consideration because of high cost. Some non-precious alloys might be used, but these need to provide the same performance as Ni-YSZ for the other electrochemical reactions.

The second approach would involve a dynamic process, whereby the sulfur is adsorbed onto the surface and then fed with oxygen, which has diffused from the air side through the electrolyte, to form SO_2, and is then desorbed and sent to the exhaust. In this case the material, presumably a metal or alloy, must preferentially adsorb sulfur over hydrogen, and thus it may be necessary to have two different metal sites, one for the hydrogen adsorption and one for sulfur. One of the current projects at ANL is studying the effects of sulfur on anode materials in an attempt to solve a challenging new problem to the development of commercial SOFC systems.

5. Bipolar plates

5.1. Ceramic bipolar plates

The bipolar plate or interconnect arguably faces the greatest materials challenge of all the SOFC components. The bipolar plate material, which is exposed to both the fuel and oxidant gases, must have a good electronic conductivity and negligible ionic conductivity. In many planar designs, the bipolar plate also facilitates the channeling of gases across each cell. The present high operating temperatures (1000°C) prevent most metals or alloys from being considered, and thus, the material of choice has been a ceramic based on the perovskite system $LaCrO_3$ [58]. Both calcium and strontium doping have been used in this material to reduce the high temperatures necessary to sinter the undoped material (1700°C) and to improve the conductivity [59]. With the reduction in operating temperatures, however, this material no longer has the desired conductivity. It is also considerably more expensive than some of the alternative materials that can now be investigated. No other ceramic systems have been found to replace the presently used lanthanum chromite and with the introduction of metallic interconnects, further research in this area appears unlikely.

5.2. Metallic bipolar plates

The move to metallic alloys is very significant because metals and alloys are structurally much more robust compared to ceramics and are much easier to form into complex shapes. This leads to the possibility that the bipolar plate may eventually be used as the support for each cell, with the anode, electrolyte, and cathode layers deposited on top of it.

The first requirement that must be met for any bipolar plate material is a close thermal expansion match to the electrolyte material. Many candidate metals and alloys have high thermal expansion coefficients, which would lead to cell cracking during thermal cycling. A second important requirement is a low cost alloy. Fortunately, both of these requirements are satisfied by the ferritic stainless steels [60]. These alloys have no problems operating on the anode side of the fuel cell and are impermeable to both oxidant and fuel gases. Being metallic, the electronic conductivity is considerably higher in these alloys compared to the doped lanthanum chromites, and there is no measurable oxygen ion conductivity. Another advantage of the metallic over the ceramic systems is their larger thermal conductivities, which should help to reduce stresses within each cell that occur due to the temperature gradients in the fuel cell stack.

The most serious problem that arises from metallic bipolar plates is that an oxide scale forms in the air atmosphere on the cathode side. The oxide scale generally has a much poorer conductivity compared to the alloy and is prone to spalling and cracking during long-term operation, which would seriously reduce the performance of a stack [61].

The ferritic stainless steels form chromia scales on oxidation, which are reasonably adherent to the alloys and provide some protection to further corrosion of the alloys. Unfortunately, the oxide scale resistivity is above the recommended value of 25 $m\Omega cm^2$ for the bipolar plate, and an alternative must be found [62]. One of the best corrosion-resistant alloying elements that can be added to ferritic stainless steel is aluminium. Unfortunately, the aluminium forms an Al_2O_3 scale that has a high electrical resistivity and should be avoided. At present, finding an alternative single material that will satisfy all the requirements of the bipolar plate appears unlikely. To solve the problem of oxidation of these alloys, two approaches can be taken. The steel alloys can either be alloyed with additional elements that increase the conductivity within the oxide scale layer, or the steel can be coated with a highly conducting oxide.

Using a newly developed tape-casting technique at ANL, one can now cheaply alloy commercially available ferritic stainless steel powders, such as 430 SS and 434 SS. The ability to easily alloy commercially available alloy powders opens up a wide matrix of potential bipolar plate materials. The oxide scale conductivity of chromia can be increased by addition of Ni^{2+} and Co^{2+} ions into the ferritic steel alloy [63]. The protective properties of chromia scales may be improved by small additions of so-called reactive elements, such as Y, La, Ce, and Zr [60, 64]. The main effects of these elements on the chromia scales are to enhance the selective formation of these scales on the alloys, improve the adherence of the chromia scales to the metal substrates, and reduce the grain size within the chromia scales. Although some attention has been directed into each of these effects, further work is still required to understand and develop bipolar plates that are stable in the long term.

The other approach under scrutiny is applying a protective coating on the ferritic stainless steels, especially

with the reactive elements La and Y and some perovskite materials (Sr- and Ca-doped $LaMnO_3$, Ca-doped $YMnO_3$, and Sr-doped $LaCoO_3$) [65]. The objective is to introduce a corrosion barrier to the alloy that has a good electrical conductivity. The technique used to apply the coating will determine the cost of this layer, but even the cheaper methods are likely to be more expensive than the alloying option discussed above. In summary, much research still needs to be performed in the search for a low-temperature bipolar plate material.

6. Cell and stack testing - the problem of sealing

6.1. Planar versus tubular

Despite the significant progress in tubular SOFC, considerable research continues on the planar SOFC design. The reason for this activity is that the planar design achieves of a higher power density. The main problem with building planar SOFC stacks has involved sealing the edges of each cell. Generally, the sealant is not compliant enough with the stack components and leads to gas crossover and, on thermal cycling, cracking of cells. The tubular design does not have these problems because it is essentially a sealess design. Also, the tubular design is inherently stronger due to the circular shape.

We are unsure which of the two designs will ultimately be successful, but it is likely that both will survive for the near term because they are being targeted at different markets. The tubular design of Siemens Westinghouse is aimed at larger scale power generation ($>$100 kW), whereas the planar designs are concentrating on small-scale power ($<$10 kW) for individual housing and auxiliary power applications.

6.2. Sealing materials

While some groups are now claiming to have solved the problem of sealing planar SOFC stacks [6, 26], no convincing data have been yet published to support this assertion. Until such information becomes available, sealing remains a serious problem in the development of the SOFC.

On a laboratory scale, both compression seals and gold gaskets have been used to seal single cells, but for a stack these are not practical. The compression seal will almost certainly lead to gas leakage because producing very flat ceramic surfaces is difficult, and the gold gaskets would become too expensive to be used on a large scale. The design adopted by Virkar *et al.* [38] utilises solid mica gaskets in the stack, which are reported to seal well.

The most widely used sealing materials are glasses, ceramics, and glass-ceramics. Pyrex is a common glass used in research laboratories [66]. Many of the sealing materials used industrially remain proprietary. Because few research institutions perform stack tests, limited data are available on suitable sealing materials, and most of the published data are for sealant materials that can function up to 1000°C. With the drive to lower operating temperatures ($<$800°C), new sealant materials will need to be developed since the lower temperatures should reduce the stresses within the stack and widen the choice of suitable materials.

A sealing material developed a few years ago at ANL was based on a SrO-La_2O_3-Al_2O_3-B_2O_3-SiO_2 glass-ceramic system [11]. This material was very flexible because the thermal expansion could be matched to that of the SOFC components, while maintaining a viscosity that was tolerant to thermal cycling, and sustaining a gas-tight seal. Long-term testing will be required to fully evaluate the performance of this material, but it will probably perform better at lower operating temperatures, where the thermal stresses are reduced.

7. Conclusions

More research is needed to optimise the performance of an SOFC operating at lower temperatures. Operation at reduced temperatures has become almost mandatory in the SOFC design if the cost of a complete system is to compete with conventional power generation. Some tough materials challenges need to be solved, especially for the anode, cathode, and bipolar plate. Reliable long-term stack testing is required to ultimately evaluate any complete system. This paper has identified current problems and techniques that are being used to solve them. The goal is to resolve the materials problems before the polymer membrane fuel cells dominate the markets. Below is a summary of the current development of the materials needed for a lower operating temperature SOFC.

7.1. Electrolytes

At present, YSZ remains the best electrolyte material for temperatures down to 700°C. To achieve acceptable performance at these lower temperatures, thinner films need to be used and thus the electrolyte can no longer be considered for the support in the planar SOFC. For temperatures below 700°C, doped-ceria is the only material choice.

7.2. Cathodes

While LSM remains the preferred cathode material for use with YSZ at high temperatures, alternative cathodes will be required for operation at lower temperatures. Several materials have been identified in this review that have the potential to replace LSM, especially at or below 800°C. Of these, $La_{0.8}Sr_{0.2}FeO_3$ exhibits the highest and most stable performance and requires further evaluation. For CGO electrolytes, substitution of the La with Sm, Gd, or Nd in the cobaltate appears to reduce the areal resistance and lower the activation energy. Also, $La_{0.8}Sr_{0.2}Co_{0.8}Fe_{0.2}O_3$ shows a reasonably good, stable performance; however, the very good performance obtained with $Gd_{0.8}Sr_{0.2}CoO_3$ makes this material an attractive candidate cathode, especially at or below 650°C.

7.3. Anodes

The Ni-YSZ cermet is likely to remain in use until a more sulfur tolerant anode can be demonstrated. Ni-YSZ anodes require virtually sulfur-free fuels to prevent poisoning of the Ni sites. This requires additional

equipment to remove sulfur from the fuel prior to it being fed into the SOFC stack. New materials/doping statergies will need to be developed for anodes so that operation using sulfur-containing fuels can be achieved, without a decrease in SOFC performance.

7.4. Bipolar plates

With the drive to operate SOFCs at lower temperatures, there will be a switch from ceramic to metallic materials for the bipolar plate. Ferritic stainless steels are the most promising alloys. The main problem for metallic bipolar plates is the formation of an oxide scale on the cathode side, which introduces a high electrical resistance into the SOFC. Alloying and applying a conducting ceramic coatings are two approaches that are being used to solve the oxide scale problem.

7.5. Sealants

A sealant that is able to withstand thermal cycling without cracking cell components has not yet been reported and remains a serious problem for the planar SOFC. A lower operating temperature should improve the selection options but more research needs to be addressed to this issue.

Acknowledgements

This research was sponsored by the U.S. Department of Energy National Energy Technology Laboratory under Contract No. W-31-109-ENG-38. The authors would especially like to thank Mr. Wayne Surdoval from the Department of Energy for his continued support of this work. The authors would also like to thank Dr. J. T. Vaughey and Dr. J. D. Carter for critically reading this manuscript and providing useful discussions. Mr. B. Stover is also thanked for the preparation and testing of some of the powders.

References

1. S. C. SINGHAL, in Proceedings of the 6th International Symposium on Solid Oxide Fuel Cells, Honolulu, October 1999, edited by S. C. Singhal and M. Dokiya (The Electrochemical Society, Inc., Pennington, NJ, 1999) p. 39.
2. R. DIETHELM, M. SCHMIDT, K. HONEGGER and E. BATAWI, in Proceedings of the 6th International Symposium on Solid Oxide Fuel Cells, Honolulu, October 1999, edited by S. C. Singhal and M. Dokiya (The Electrochemical Society, Inc., Pennington, NJ, 1999) p. 60.
3. N. Q. MINH, C. R. HORNE, F. LIU, P. R. STASZAK, T. L. STILLWAGON and J. J. VAN ACKEREN, in Proceedings of the 1st International Symposium on Solid Oxide Fuel Cells, Hollywood, October 1989, edited by S. C. Singhal (The Electrochemical Society, Inc., Pennington, NJ, 1989) p. 307.
4. H. MORI, H. OMURA, N. HISATOME, K. IKEDA and K. TOMIDA, in Proceedings of the 6th International Symposium on Solid Oxide Fuel Cells, Honolulu, October 1999, edited by S. C. Singhal and M. Dokiya (The Electrochemical Society, Inc., Pennington, NJ, 1999) p. 52.
5. B. GODFREY, R. GILLESPIE and K. FOEGER, in Proceedings of the 6th International Symposium on Solid Oxide Fuel Cells, Honolulu, October 1999, edited by S. C. Singhal and M. Dokiya (The Electrochemical Society, Inc., Pennington, NJ, 1999) p. 75.
6. http://www.globalte.com/index.htm
7. E. PONTHIEU, in Proceedings of the 6th International Symposium on Solid Oxide Fuel Cells, Honolulu, October 1999, edited by S. C. Singhal and M. Dokiya (The Electrochemical Society, Inc., Pennington, NJ, 1999) p. 19.
8. S. J. VISCO, C. JACOBSON and L. C. DE JONGHE, in Proceedings of the 5th International Symposium on Solid Oxide Fuel Cells, Aachen, June 1997, edited by U. Stimming, S. C. Singhal, H. Tagawa and W. Lehnert (The Electrochemical Society, Inc., Pennington, NJ, 1999) p. 710.
9. N. Q. MINH, *J. Amer. Ceram. Soc.* **76**(3) (1993) 563.
10. J. P. ACKERMAN and J. E. YOUNG, U.S. Patent no. 4,476,196, Oct. 9, 1984.
11. K. L. LEY, M. KRUMPELT, R. KUMAR, J. H. MEISER and I. BLOOM, *J. Mater. Res.* **11**(6) (1996) 1489.
12. R. DOSHI, V. L. RICHARDS, J. D. CARTER, X. WANG and M. KRUMPELT, *J. Electrochem. Soc.* **146**(4) (1999) 1273.
13. S. TERAUCHI, H. TAKIZAWA, T. ENDO, S. UCHIDA, T. TERUI and M. SHIMADA, *Mat. Letts.* **23** (1995) 273.
14. L. G. COCCIA, G. C. TYRRELL, J. A. KILNER, D. WALLER, R. J. CHATER and I. W. BOYD, *Appl. Surf. Sci.* **96–98** (1996) 795.
15. M. SAHIBZADA, B. C. H. STEELE, K. ZHENG, R. A. RUDKIN, J. M. BAE, N. KIRATZIS, D. WALLER and I. S. METCALFE, in Proceedings of the 2nd European Solid Oxide Fuel Cell Forum, Oslo, May 1996, edited by B. Thorstensen (European Solid Oxide Fuel Cell Forum, 1996) p. 687.
16. J.-F. JUE, J. JUSKO and A. V. VIRKAR, *J. Electrochem. Soc.* **139** (9) (1992) 2458.
17. B. C. H. STEELE, *Current Opinion in Solid State and Material Science* **1** (1996) 684.
18. *Idem.*, in Proceedings of the 1st European Solid Oxide Fuel Cell Forum, Lucerne, October 1994, edited by U. Bossel (European Solid Oxide Fuel Cell Forum, 1994) p. 375.
19. P. D. BATTLE, C. R. A. CATLOW, J. DRENNAN and A. D. MURRAY, *J. Phys. C: Sol. State Phys.* **16** (1983) L561.
20. T. TAKAHASHI, T. ESAKA and H. IWAHARA, *J. Appl. Electrochem.* **7** (1977) 299.
21. J. M. RALPH, Ph.D. Thesis, University of London, 1998.
22. F. A. KROEGER and H. J. VINK, *Solid State Physics* **3** (1956) 307.
23. M. SAHIBZADA, S. J. BENSON, R. A. RUDKIN and J. A. KILNER, *Solid State Ionics* **113–115** (1998) 285.
24. S. J. VISCO, C. JACOBSON and L. C. DE JONGHE, in Proceedings of the 6th International Symposium on Solid Oxide Fuel Cells, Honolulu, October 1999, edited by S. C. Singhal and M. Dokiya (The Electrochemical Society, Inc., Pennington, NJ, 1999) p. 861.
25. K. HONEGGER, R. KRUSCHWITZ, M. KELLER and G. M. CHRISTIE, in Proceedings of the 6th International Symposium on Solid Oxide Fuel Cells, Honolulu, October 1999, edited by S. C. Singhal and M. Dokiya (The Electrochemical Society, Inc., Pennington, NJ, 1999) p. 1019.
26. N. MINH, A. ANUMAKONDA, B. CHUNG, R. DOSHI, J. FERRALL, J. GUAN, G. LEAR, K. MONTGOMERY, E. ONG and J. YAMANIS, in Proceedings of the 6th International Symposium on Solid Oxide Fuel Cells, Honolulu, October 1999, edited by S. C. Singhal and M. Dokiya (The Electrochemical Society, Inc., Pennington, NJ, 1999) p. 68.
27. T. ISHIHARA, H. MATSUDA and Y. TAKITA, *J. Amer. Chem. Soc.* **116** (1994) 3801.
28. M. FENG and J. B. GOODENOUGH, *Eur. J. Solid State Inorg. Chem.* **t31** (1994) 663.
29. J. WOLFENSTINE, P. HUANG and A. PETRIC, *Solid State Ionics* **118** (1999) 257.
30. Y. MIZUTANI, M. KAWAI, K. NOMURA, Y. NAKAMURA and O. YAMAMOTO, in Proceedings of the 5th International Symposium on Solid Oxide Fuel Cells, Aachen, June 1997, edited by U. Stimming, S. C. Singhal, H. Tagawa and W. Lehnert (The Electrochemical Society, Inc., Pennington, NJ, 1999) p. 196.
31. A. MITTERDORFER and L. J. GAUCKLER, *Solid State Ionics* **111** (1998) 185.
32. T. KAWADA, N. SAKAI, H. YOKOKAWA, M. DOKIYA and I. ANZAI, *ibid.* **50** (1992) 189.
33. R. A. DE SOUZA and J. A. KILNER, *ibid.* **106** (1998) 175.

34. Z. LI, M. BEHRUZI, L. FUERST and D. STÖVER, in Proceedings of the 3rd International Symposium on Solid Oxide Fuel Cells, Honolulu, May 1993, edited by S. C. Singhal and H. Iwahara (The Electrochemical Society, Inc., Pennington, NJ, 1993) p. 171.
35. G. STOCHNIOL, E. SYSKAKIS and A. NAOUMIDIS, *J. Amer. Ceram. Soc.* **78**(4) (1995) 929.
36. J. W. STEVENSON, T. R. ARMSTRONG and W. J. WEBER, in Proceedings of the 4th International Symposium on Solid Oxide Fuel Cells, Yokohama, June 1995, edited by M. Dokiya, O. Yamamoto, H. Tagawa and S. C. Singhal (The Electrochemical Society, Inc., Pennington, NJ, 1995) p. 454.
37. T. TSAI and S. A. BARNETT, in Proceedings of the 5th International Symposium on Solid Oxide Fuel Cells, Aachen, June 1997, edited by U. Stimming, S. C. Singhal, H. Tagawa and W. Lehnert (The Electrochemical Society, Inc., Pennington, NJ, 1997) p. 368.
38. J.-W. KIM, A. V. VIRKAR, K.-Z. FUNG, K. MEHTA and S. C. SINGHAL, *J. Electrochem. Soc.* **146**(1) (1999) 69.
39. X. WANG, J. RALPH, J. VAUGHEY and M. KRUMPELT, Presented at the 1999 Joint DOE/EPRI/GRI Fuel Cell Technology Review Conference, Chicago, IL, August, 1999. To be published on CD-ROM.
40. V. V. KHARTON, A. A. YAREMCHENKO and A. N. NAUMOVICH, *J. Solid State Electrochem.* **3** (1999) 303.
41. O. YAMAMOTO, Y. TAKEDA, R. KANNO and M. NODA, *Solid State Ionics* **22** (1987) 241.
42. C. S. TEDMON, JR., H. S. SPACIL and S. P. MITOFF, *J. Electrochem. Soc.* **116** (9) (1969) 1170.
43. Y. TAKEDA, H. Y. TU, H. SAKAKI, S. WATANABE, N. IMANISHI, O. YAMAMOTO, M. B. PHILLIPPS and N. M. SAMMES, *ibid.* **144**(8) (1997) 2810.
44. H. Y. LEE, J. H. JANG and S. M. OH, *ibid.* **146**(5) (1999) 1707.
45. G. C. KOSTOGLOUDIS and C. FTIKOS, *J. Euro. Ceram. Soc.* **19** (1999) 497.
46. T. ISHIHARA, M. HONDA, T. SHIBAYAMA, H. MINAMI, H. NISHIGUCHI and Y. TAKITA, *J. Electrochem. Soc.* **145**(9) (1998) 3177.
47. G. C. KOSTOGLOUDIS, P. FERTIS and C. FTIKOS, *J. Euro. Ceram. Soc.* **18** (1998) 2209.
48. E. IVERS-TIFFÉE, M. SCHIEßL, H. J. OEL and W. WERSING, in Proceedings of the 14th Risø International Symposium on High Temperature Electrochemical Behaviour of Fast Ion and Mixed Conductors, Risø, September 1993, edited by F. W. Poulsen, J. J. Bentzen, T. Jacobsen, E. Skou and M. J. L. Østergård (Risø National Laboratory, Denmark, 1993) p. 69.
49. H. SCHACHNER and H. TANNENBERGER, in Proceedings of the 1st International Symposium on Fuel Cells, Bruxelles, 1965, Volume III, p. 19.
50. Westinghouse Electric Corp., Final Report, Project Fuel Cell, Rep. No. 57 (1970).
51. D. W. DEES, T. D. CLAAR, T. E. EASLER, D. C. FEE and F. C. MRAZEK, *J. Electrochem. Soc.* **134**(9) (1987) 2141.
52. R. MARIC, S. OHARA, T. FUKUI, T. INAGAKI and J. FUJITA, *Electrochemical and Solid State Letts.* **1**(5) (1998) 201.
53. J. P. KOPASZ, R. WILKENHOENER, S. AHMED, J. D. CARTER and M. KRUMPELT, in Proceeding of the 218th ACS National Meeting, New Orleans, August 1999, edited by J. A. Franz, p. 889.
54. S. AHMED, J. P. KOPASZ, B. J. RUSSELL and H. L. TOMLINSON, to be published in the Proceedings of the 3rd International Fuel Cell Conference, Nagoya, Japan, Nov.-Dec., 1999.
55. S. AHMED, M. KRUMPELT, R. KUMAR, S. H. D. LEE, J. D. CARTER, R. WILKENHOENER and C. MARSHALL, in Extended Abstracts of the Fuel Cell Seminar, Palm Springs, November 1998, edited by A. Pittman and H. Gavilan (Courtesy Associates, Inc., 1998) p. 242.
56. American Petroleum Institute, "Fuel Choices for Fuel Cell Powered Vehicles" (API, Washington, D.C., 2000) p. 14.
57. S. C. SINGHAL, Private communications.
58. H. YOKOKAWA, N. SAKAI, T. KAWADA and M. DOKIYA, *J. Electrochem. Soc.* **138**(4) (1991) 1018.
59. N. SAKAI, T. KAWADA, H. YOKOKAWA and M. DOKIYA, in Proceedings of the 2nd International Symposium on Solid Oxide Fuel Cells, Athens, July 1991, edited by F. Grosz, P. Zegers, S. C. Singhal and O. Yamamoto (Commission of the European Communities, 1991) p. 629.
60. P. KOFSTAD, in Proceedings of the 2nd European Solid Oxide Fuel Cell Forum, Oslo, May 1996, edited by B. Thorstensen (European Solid Oxide Fuel Cell Forum, 1996) p. 479.
61. D. ENGLAND and A. V. VIRKAR, *J. Electrochem. Soc.* **146** (9) (1999) 3196.
62. S. LINDEROTH, P. V. HENDRIKSEN and M. MOGENSEN, *J. Mater. Sci.* **31**(19) (1996) 5077.
63. A. I. SAPRYKIN, J. S. BECKER, U. V. D. CRONE and H.-J. DIETZE, *Fresenius J. Anal. Chem.* **358** (1997) 145.
64. P. Y. HOU and J. STRINGER, *Mat. Sci. Eng.* **A202** (1995) 1.
65. G. SCHILLER, R. HENNE and R. RUCKDASCHEL, *J. Adv. Mat.* **32**(1) (2000) 3.
66. M. MORI, Y. HIEI, T. YAMAMOTO and H. ITOH, *J. Electrochem. Soc.* **146**(11) (1999) 4041.

Received 2 May
and accepted 14 June 2000